IUST
Iran University of Science and Technology

Iranian Journal of Electrical and Electronic Engineering

Journal Homepage: ijeee.iust.ac.ir

Research Paper

Criteria for Choosing of Resonant Circuit Parameters of Wireless Power Transfer Charging System

V. M. Zavylov*, I. Y. Semykina**(C.A.), S. A. Abeidulin*, E. A. Dubkov*, and A. S. Veliliaev*

Abstract: The promising element of the infrastructure of unmanned electric vehicles is wireless chargers. The central part of such systems is a resonant circuit that provides wireless power transfer. The article discusses a set of criteria used for making the rational choice of the resonant circuit parameters. Such criteria include the efficiency, the current transfer coefficient, the excess voltage on the resonant circuit capacitors over the input voltage, the ratio between the transmitting circuit current and the receiving one. For the resonant circuit with fixed coils size and fixed resonant frequency, the families of curves were obtained via parametric analysis to show how these criteria change depending on the inductance and capacitance of the resonant circuit. The obtained dependencies allow choosing the rational inductances and capacitances of the resonant circuit, providing for a given size and a given value of the input voltage the highest conveyed power with the highest efficiency at the minimum voltage class of capacitors and the minimum current of semiconductor switches. The results of the parametric analysis were confirmed experimentally.

Keywords: Battery, Resonant Circuit, Transmitting and Receiving Coils, Unmanned Electric Vehicle, Wireless Charger, Wireless Power Transfer.

1 Introduction

IN recent years, the intensive development of electrochemical energy sources, power electronics, artificial intelligence, etc. have shaped the development of unmanned electric vehicles. Successful implementation of such vehicles in everyday life depends on a number of factors, including the creation of supporting infrastructure. One of the most important elements of this infrastructure is the system of charging stations, and it is desirable that such stations be automated and do not require human participation. From this point of view, the most promising are charging stations with wireless power transfer (WPT).

Various authors consider the features of using charging stations with WPT for electric vehicles [1-4], drones [5, 6], and underwater vehicles [6]. When using a wireless charger, the vehicle only needs to arrive at the location point where the transmitting coil is located and does not need to use human assistance.

The central part of the wireless charger is a resonant circuit. There are four main topologies of resonant circuits considered in [4, 7, 8] that are combinations of series and parallel connection of capacitors with the transmitting and receiving coils. As a current source is required for battery charging, the most suitable topology for the resonant circuit of wireless charger seems to be the series connection of capacitors in the primary and secondary sides [7].

One of the most urgent research areas for wireless chargers is choosing and optimization of their parameters. Many works consider their constructive optimization, for instance, the analysis of how the coils' geometry influences the energy efficiency of wireless chargers [9-11], or the analysis of changes in the coils relative position [12-14]. The hallmark of the

Iranian Journal of Electrical and Electronic Engineering, 2022.
Paper first received 15 July 2021, revised 18 September 2021, and accepted 26 September 2021.
* The authors are with the Department of Electric Power Systems of Nuclear Plants, Sevastopol State University, Sevastopol, Russia.
E-mails: vmzavyalov@sevsu.ru, saabeidulin@sevsu.ru, eadubkov@sevsu.ru, and velilyaev1999@bk.ru.
** The author is with the Educational and Scientific Center of Information Technologies of Education, Sevastopol State University, Sevastopol, Russia.
E-mail: arinasemykina@gmail.com.
Corresponding Author: I. Y. Semykina.
https://doi.org/10.22068/IJEEE.18.1.2236

considered wireless chargers is the dependence of their energy efficiency on the load resistance. To optimize the energy efficiency under variable load, the paper [15] proposes a step-change in the resonant frequency by switching a capacitor bank in the resonant circuit. Other works [16, 17] investigate the optimization of energy efficiency by using several resonant circuits on the secondary side for a given coil geometry and a given resonant frequency.

In contrast to the above works, this paper considers a set of criteria that help to choose the parameters of the resonant circuit not optimally but rationally.

When designing wireless chargers, a multi-criteria task is solved. On the one hand, it is necessary to ensure the highest energy efficiency of WPT, and on the other hand, there is a need to fulfill some restrictions on weight and size characteristics, on an allowable voltage across capacitors, on operating frequency range, and others. To solve this task, the following criteria are proposed:

1) The efficiency η, showing the energy efficiency of WPT;
2) The current transfer coefficient k_i, showing the ratio of the load current, which is equal to receiving circuit current, to the input voltage that characterizes the power conveyed to the load at the fixed input voltage;
3) The coefficient of excess voltage on the primary side capacitor over the input voltage k_{C1} and the same on the secondary side capacitor k_{C2}, characterizing the voltage class of these capacitors;
4) The ratio between the transmitting circuit current and the receiving circuit current a_i that characterizes the maximum current of the semiconductor switching elements of the wireless charger.

For rational choosing of inductances and capacitances of the resonant circuit, it is necessary to study their influence on the above criteria. The study will be carried out with the fixed geometry of the resonant circuit coils, the fixed resonant frequency, under varied values of the inductances and capacitances, as well as the equivalent resistance of the load.

2 Theory

2.1 Models and Approaches

The functional diagram of the wireless charger with the topology of the series connection of capacitors is shown in Fig. 1. In this system, the supplied voltage from the industrial AC grid is rectified and converted by an inverter into an input voltage with the resonant frequency. This high-frequency voltage feeds the resonant circuit with the transmitting and receiving coils. The voltage of the receiving circuit is converted by a rectifier into direct current, which is necessary to charge the battery.

It should be noted that the resonant frequency of the

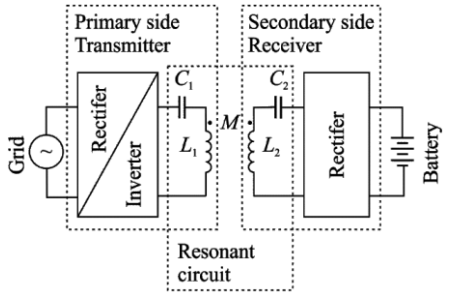

Fig. 1 Functional diagram of the wireless charger.

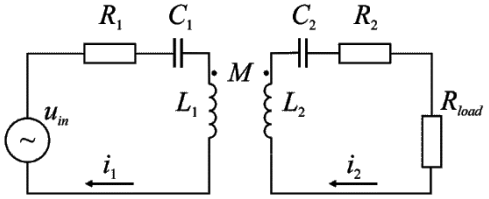

Fig. 2 Idealized equivalent circuit of the wireless charger.

wireless charger f_r is in the range of megahertz and its value depends on the resonant circuit parameters. If the frequency of the input voltage f does not correspond to the resonant value, the wireless charger will not be able to convey to the load as much power as possible. To evaluate the conveyed power in that case so-called resonant curves showing the dependence of the receiving circuit current i_2 on the frequency f at the fixed input voltage u_{in} are used. The shape of the resonant curves depends on the coupling coefficient between the coils that is determined by the ratio:

$$K = \frac{M}{\sqrt{L_1 L_2}},$$

where L_1, L_2 are transmitting and receiving coils inductance consequently; M is mutual inductance.

In the case of weak coupling where K is less than the critical value the power in the receiving circuit significantly lower than the power given by the transmitting circuit. The resonance curve has one extremum. In the case of strong coupling, the backreaction of the receiving circuit to the transmitting one becomes significant, and the resonance curve acquires two extrema. Operating of the wireless charger in the condition of strong coupling is more efficient so the resonant circuit parameters should provide it.

The analytical study of the presented wireless charger uses the idealized equivalent circuit of the wireless charger operating on a resistive load as shown in Fig. 2. This equivalent circuit contains the following assumptions: the power source is ideal; capacitors losses are neglected; actual inverter characteristics are not taken into account; the inverter output voltage is sinusoidal; the load is purely active; the displacement current effect in conductors is not taken into account. Despite the mentioned assumptions, this equivalent circuit allows analyzing the main characteristics and

dependencies of the system.

The idealized equivalent circuit of the wireless charger is described by the following differential equations of the fourth-order:

$$u_{in} = u_{C1} + i_1 R_1 + L_1 \frac{di_1}{dt} + M\left(\frac{di_1}{dt} + \frac{di_2}{dt}\right);$$
$$0 = u_{C2} + L_2 \frac{di_2}{dt} + M\left(\frac{di_1}{dt} + \frac{di_2}{dt}\right) + i_2 R_{2\Sigma};$$
$$i_1 = C_1 \frac{du_{C1}}{dt}; \quad i_2 = C_2 \frac{du_{C2}}{dt}. \tag{1}$$

where u_{in} is the input voltage; u_{C1} is the capacitor voltage at the primary side; u_{C2} is the capacitor voltage at the secondary side; i_1 is the transmitting circuit current; i_2 is the receiving circuit current that is equal to the load current; R_1, R_2, C_1, C_2 are primary side and secondary side resistance and capacitance consequently; R_{load} is the equivalent resistance of the battery; $R_{2\Sigma}$ is sum ($R_2 + R_{load}$).

According to model (1), the proposed criteria are calculated by:

$$k_i = \frac{i_2}{u_{in}}; \; k_{C1} = \frac{u_{C1}}{u_{in}}; \; k_{C2} = \frac{u_{C2}}{u_{in}}; \; a_i = \frac{i_1}{i_2};$$
$$\eta = \frac{i_2^2 R_{load}}{\mathrm{Re}\left(i_1 u_{in}\right)}. \tag{2}$$

Since obtaining a rigorous analytical solution of the differential equation (1) with harmonic input signals is a complicated mathematical problem, to calculate (2) and analyze the resonant circuit parameters of the wireless charger, we will use the model in the Laplace-domain.

To begin with, consider the current transfer coefficient k_i characterizing the conveyed power which allows us to obtain the value of the resonant frequency. Using (1) and Laplace transform, a structural diagram was composed where the input is the input voltage u_{in} and the output is the load current i_2. This structural diagram is shown in the first line of Table 1 and the corresponding transfer function is as follow:

$$W_{k_i}(s) = \frac{i_2(s)}{u_{in}(s)},$$

where s is Laplace operator, $i_2(s) = s^3 C_1 C_2 M$, and $u_{in}(s) = C_1C_2(L_1L_2 - M)s^4 + C_1C_2(R_1L_2 + R_{2\Sigma}L_1)s^3 + (C_1C_2R_1R_{2\Sigma} + C_1L_1 + C_2L_2)s^2 + (C_1R_1 + C_2R_{2\Sigma})s + 1$.

In the following, the transfer function W_{ki} was transformed into the frequency domain by replacing s with $j\omega$ after which the real part and the imaginary part were got:

$$W_{k_i}(j\omega) = \mathrm{Re}_{k_i}(\omega) + j\,\mathrm{Im}_{k_i}(\omega),$$

where $\mathrm{Re}_{k_i}(\omega) = \frac{\mathrm{Re}_1(\omega)}{\mathrm{Re}_2(\omega)}$, $\mathrm{Re}_1(\omega) = \omega^4 C_1C_2M\left[C_1R_1 + C_2R_{2\Sigma} - \omega^2\left(C_1C_2(R_1L_2 + R_{2\Sigma}L_1)\right)\right]$, $\mathrm{Re}_2(\omega) = \left[\omega^4 C_1C_2\left(L_1L_2 - M^2\right) - \omega^2\left(C_1C_2R_1R_{2\Sigma} + C_1L_1 + C_2L_2\right) + 1\right]^2 + \left[\omega\left(C_1R_1 + C_2R_{2\Sigma}\right) - \omega^3\left(C_1C_2(R_1L_2 + R_{2\Sigma}L_1)\right)\right]^2$, $\mathrm{Im}_{k_i}(\omega) = \frac{\mathrm{Im}_1(\omega)}{\mathrm{Im}_2(\omega)}$, $\mathrm{Im}_1(\omega) = \omega^3 C_1C_2M\left[\omega^4 C_1C_2\left(L_1L_2 - M^2\right) - \omega^3\left(C_1C_2(R_1L_2 + R_{2\Sigma}L_1)\right)\right]$, $\mathrm{Im}_2(\omega) = \left[\omega^4 C_1C_2\left(L_1L_2 - M^2\right) - \omega^2\left(C_1C_2R_1R_{2\Sigma} + C_1L_1 + C_2L_2\right) + 1\right]^2 + \left[\omega\left(C_1R_1 + C_2R_{2\Sigma}\right) - \omega^3\left(C_1C_2(R_1L_2 + R_{2\Sigma}L_1)\right)\right]^2$.

The obtained equations were used in further transformation of W_{ki} to get the amplitude-frequency response and phase-frequency response:

$$A_{k_i}(\omega) = \sqrt{\mathrm{Re}_{k_i}(\omega)^2 + \mathrm{Im}_{k_i}(\omega)^2}, \tag{3}$$
$$\varphi_{k_i}(\omega) = \arctan\frac{\mathrm{Im}_{k_i}(\omega)}{\mathrm{Re}_{k_i}(\omega)}. \tag{4}$$

The complete equations of which are omitted due to their excessive cumbersomeness.

Analysis of (3) and (4) considering their complete equations is only possible by using of graphical approach. Thus for each set of the resonant circuit parameters the Bode plot of the current transfer coefficient k_i needs to be drawn where analogically to the resonant curves the resonant frequencies and the response magnitudes on them can be visually determined.

The other criteria were considered with a similar approach. Firstly, the corresponding structural diagrams were drawn and after that, their transfer functions were composed. The results are given in Table 1. Thereafter these transfer functions were transformed into the frequency domain and its real and imaginary parts were calculated. The obtained equations are omitted as they have similar complicity to the above example. Real and imaginary parts were used to get corresponding amplitude-frequency and phase-frequency responses which were analyzed graphically.

2.2 Parametric Analysis

Transfer functions (5)-(8) and their derived elements were used to conduct a parametric analysis of the wireless charger with the following parameters:

- Required resonant frequency is 90 kHz that based on the recommendation of the standard [18];
- The transmitting and receiving coils have a flat square shape with an outer coil dimension of 600×600 mm;
- The coils are located one above the other in

Table 1 Structural diagrams and transfer functions for the criteria.

Criterion	Description		
k_i	Structural diagram	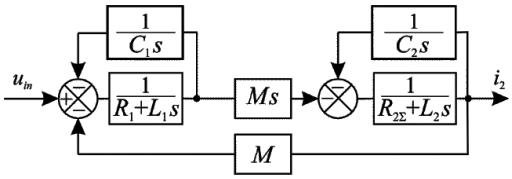	
	Transfer function	$W_{k_i}(s)=\frac{i_2(s)}{u_{in}(s)}=\frac{s^3C_1C_2M}{C_1C_2(L_1L_2-M)s^4+C_1C_2(R_1L_2+R_{2\Sigma}L_1)s^3+(C_1C_2R_1R_{2\Sigma}+C_1L_1+C_2L_2)s^2+(C_1R_1+C_2R_2)s+1}$	(5)
k_{C1}	Structural diagram	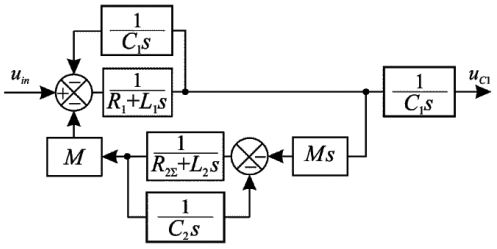	
	Transfer function	$W_{k_{C1}}(s)=\frac{u_{C1}(s)}{u_{in}(s)}=\frac{C_2L_2s^2+C_2R_{2\Sigma}s+1}{C_1C_2L_1L_2s^4+C_1C_2\left(L_2R_1+L_1R_{2\Sigma}\right)s^3+\left(C_1C_2R_1R_{2\Sigma}+C_1L_1+C_2L_2\right)s^2+\left(C_1R_1+C_2R_{2\Sigma}\right)s+2}$	(6)
k_{C2}	Structural diagram	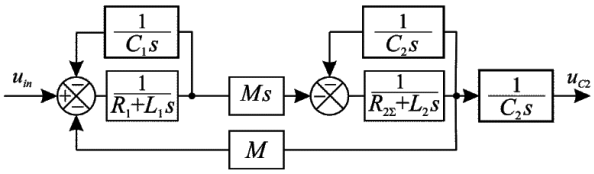	
	Transfer function	$W_{k_{C2}}(s)=\frac{u_{C2}(s)}{u_{in}(s)}=-\frac{MC_1s^2}{C_1L_1C_2L_2s^4+C_1C_2\left(R_1L_2+L_1R_{2\Sigma}-M^2\right)s^3+\left(C_1R_1C_2R_{2\Sigma}+C_1L_1+C_2L_2\right)s^2+\left(C_1R_1+C_2R_{2\Sigma}\right)s+1}$	(7)
a_i	Structural diagram	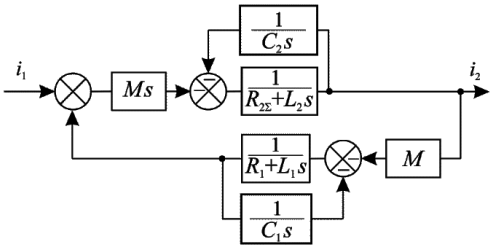	
	Transfer function	$W_{a_i}(s)=\frac{i_2(s)}{i_1(s)}=\frac{MC_1\left(C_2s\left(R_{2\Sigma}+L_2s\right)+1\right)s^2}{C_1C_2L_1L_2s^4+C_1C_2\left(L_2R_1+L_1R_{2\Sigma}+M^2\right)s^3+\left(C_1C_2R_1R_{2\Sigma}+C_1L_1+C_2L_2\right)s^2+\left(C_1R_1+C_2R_{2\Sigma}\right)s+1}$	(8)

parallel planes at a distance of 150 mm;

- Input voltage u_{in} is 24 V;
- The wireless charger capacity P_{WPT} is 500 W.

The coils under analysis were with the turn number from 1 to 10 and for each of them, the resonant circuit inductances were calculated.

The coils inductances L_1 and L_2 were obtained according to [19] as follow:

$$L_1 = L_2 = \frac{2}{\pi}\mu_0 wc\left[\ln\frac{c}{r_w}-0.524+(w-1)\left(\ln\frac{c}{p}-0,774\right)+0,178\frac{p}{c}(w^2-1)+w(w^2-1)\cdot 0,125\frac{p^2}{c^2}-wf_w\right], \quad (9)$$

where μ_0 is the magnetic constant; w is the turn number of a coils' winding; c is the side of the middle turn of the coil; r_w is the bare wire radius; p is coils' winding pitch; f_w is the function of the turn number with a tabular value.

The mutual inductance of the coils was calculated based on [20] for the case when they are coaxial:

$$M=\frac{\mu_0}{\pi}\sum_{k=\pm1}\left(\int_{x_1=0}^{c/2}\int_{x_2=-c/2}^{c/2}\frac{k\cdot dx_1\cdot dx_2}{\sqrt{\left(x_1-x_2\right)^2+0,25\left(kc-c\right)^2+h^2}}\int_{y_1=0}^{c/2}\int_{y_2=-c/2}^{c/2}\frac{k\cdot dy_1\cdot dy_2}{\sqrt{\left(y_1-y_2\right)^2+0,25\left(kc-c\right)^2+h^2}}\right), \quad (10)$$

where h is the distance between the coils.

After determining the resonant circuit inductances, based on the required wireless charger capacity and the load voltage, the equivalent resistance of the battery R_{load} was determined, and also, based on the coils wire's length and cross-section with different turn numbers their active resistances that were calculated as follow:

$$R_1 = R_2 = \rho \frac{l_w}{S} \cdot \frac{r_w^2}{2r_w \sqrt{\frac{\rho}{\pi f \mu}} - \frac{\rho}{\pi f \mu}},$$

where ρ is the electrical resistivity; l_w is the wire length; S is the cross-section area of the wire; μ is the magnetic permeability.

To provide the resonant frequency on the required value for coils with different turn numbers, the capacitances of the primary side and secondary side capacitors C_1 and C_2 were selected. The initial value of the capacitance was determined by the expression:

$$C_1 = \frac{1}{\omega^2 L_1}, \quad C_2 = \frac{1}{\omega^2 L_2}$$

after which, according to (3) and (4) with the calculated above parameters the amplitude-frequency response and the phase-frequency response were got and the Bode plot for the current transfer coefficient k_i was drawn.

The example of the Bode plot is shown in Fig. 3. As can be seen, the amplitude-frequency response has two maxima, consequently, when calculating the wireless charger the strong coupling between the transmitting and receiving coils was managed to provide. In what follows, the frequency corresponding to the first maximum was considered as the resonant frequency f_r. If the obtained resonant frequency differed from the required value, which is 90 kHz in the wireless charger under analysis, the capacitances C_1 and C_2 were selected by the method of successive approximations until the values of resonant frequencies have coincided.

As the result, the capacitances and inductances of the resonant circuit for a different turn number of coils are given in Table 2.

Taken the obtained parameters L_1, L_2, M, C_1, and C_2 of the resonant circuit, for the criteria k_{C1}, $k_{C2,}$ and a_i the Bode plots were drawn and the value of magnitude and phase for the criterion at the resonant frequency was fixed on each plot. For the given input voltage u_{in} the coefficient k_i and the ratio a_i provide calculating of the efficiency η as follow:

$$\eta = \frac{k_i^2 R_{load}}{k_i a_i \cos\varphi},$$

where φ is the angle between the input voltage u_{in} and the transmitting circuit current i_1 that is determined from the phase plots of the current transfer coefficient k_i and the ratio between the transmitting circuit current and the receiving circuit current a_i:

$$\varphi = \varphi_{k_i} - \varphi_{a_i}.$$

Described procedure was carried out for various equivalent resistances of the load and allowed us to draw families of curves at Fig. 4 that show how the criteria change depending on transmitting and receiving coils inductance $L = L_1 = L_2$.

These curves indicate that coefficient k_i is nonlinear and decreases with the increase of the inductance L that means if the inductance L declines the conveyed power of the wireless charger rises. However, too small inductance L contributes to a decrease in the efficiency η because of the large excess of transmitting coil current and consequently increased power losses in this coil.

The coefficients k_{C1} and k_{C2} have the best values when the efficiency η is maximum, i.e. the optimal energy efficiency coincides with the minimum voltage class of capacitors.

It should also be noted that as R_{load} decreases which corresponds to the load capacity increase the lower inductance L is required to ensure the optimum of energy efficiency and therefore the transmitting and receiving coils might be with the smaller turn number. At the same time, reduction of R_{load} corresponds to restriction of the area around the extremum, making the optimum of energy efficiency more pronounced.

Since the initial equations (1) is a system of linear differential equations, the analysis of the shown families

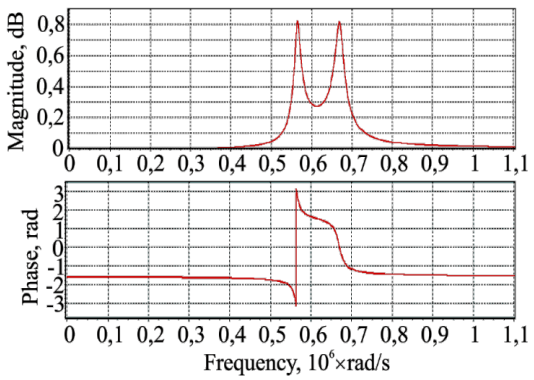

Fig. 3 Bode plot for the current transfer coefficient k_i.

Table 2 Capacitance and inductance of the resonant circuit with the different turn numbers of coils.

Turn number	Resonant circuit parameter		
	$L = L_1 = L_2$ [μH]	M [μH]	$C_1 = C_2$ [nF]
1	5	0.41	626
2	13	1.6	227
3	23	3.5	123
4	35	6	76.7
5	48	9	55
6	61	12.4	42.7
7	76	16.2	34
8	90	20.3	28.4
9	105	24.6	24.2
10	120	29	21

of curves made it possible to algorithmize the general procedure for optimization of the resonant circuit parameters of any wireless charger by the means of the flowchart shown in Fig. 5.

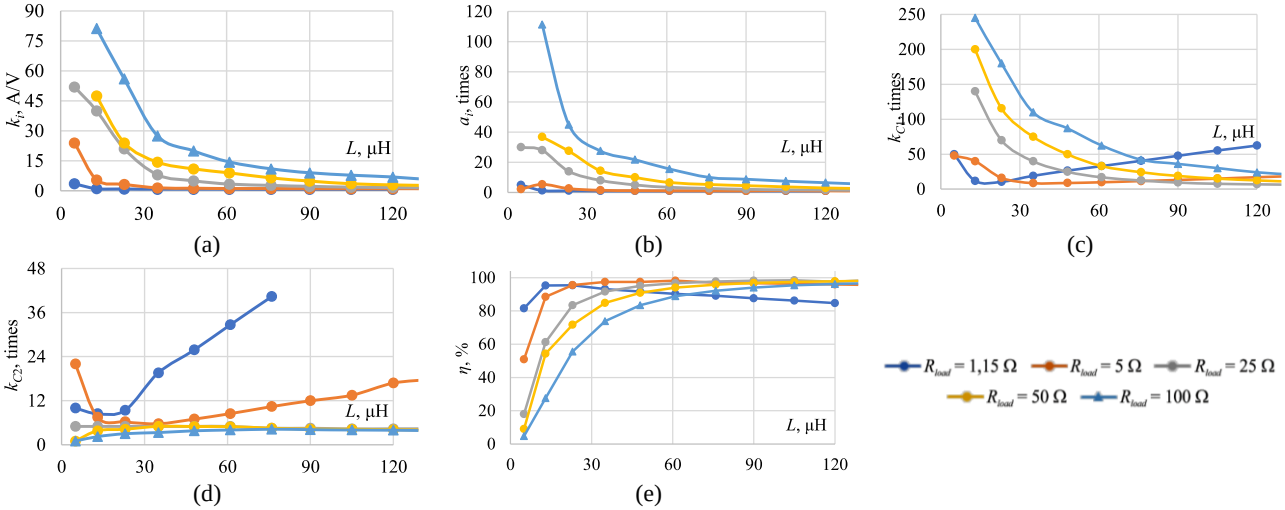

Fig. 4 Families of curves indicating dependences of the criteria on the inductance L for different values of R_{load}.

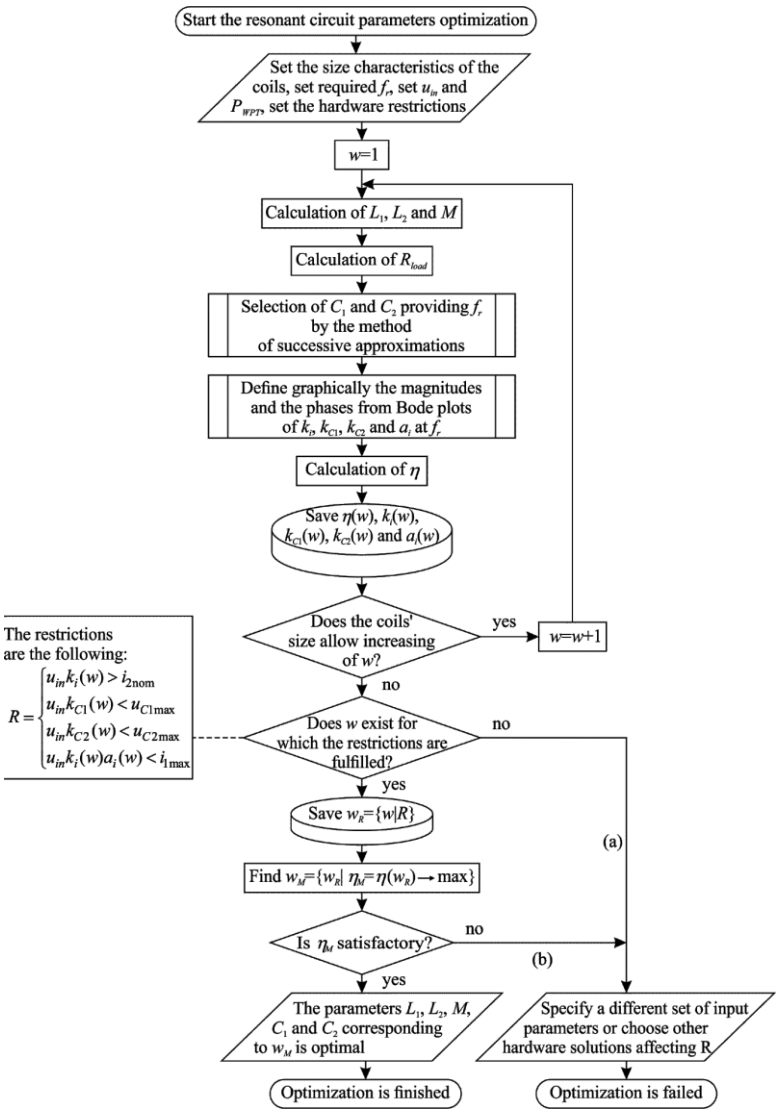

Fig. 5 Flowchart the resonant circuit parameters optimization.

It should be noted that it is incorrect to call as optimal the parameters obtained as a result of the successful execution of this algorithm in the strict mathematical sense since an optimality criterion has not been set analytically and the search for a solution is carried out using a graph-analytical approach, which allows errors due to the human factor. The more correct name for the algorithm, in this case, is rational choosing of inductances and capacitances of the resonant circuit, and the term "optimization" has been used for brevity and clarification of what the authors mean by "rational choosing".

It should be separately discussed the probable reasons why the execution of the optimization algorithm might be unsuccessful. The first group of reasons, marked with letter (a) on the flowchart, relates to the hardware solutions of the wireless charger, such as the choice of the type for capacitors or semiconductor switching elements. To rectify the situation, capacitors of the same capacity should be chosen, but with a higher voltage class, or power transistors with the same rated current should be implemented, but with a higher maximum current. If these measures are not enough, the value of the input voltage should be changed.

The second group of reasons, marked with letter (b) on the flowchart, is responsible for low efficiency. First, it could be too small linear dimensions of the coils at a high desired power conveyed to the load or a very large distance between the coils. The last-mentioned factor is even more significant since the coupling coefficient between the coils K and the energy efficiency of WPT depend on this distance to a large extent. According to [21, 22], the wireless charger has an efficiency of more than 90% if, the first, it operates in the resonant mode, the second, the distances between coils is below the threshold where coupling between the coils become weak that does not allow efficient WPT. If the reason for unsatisfactory efficiency η is weak coupling, the distance between the coils should be reduced.

Second, incorrect hardware solutions might affect efficiency undervaluing it. This can happen if due to the restrictions R the turn number of coils and therefore the inductance L turns out to be too low and the wireless charger will work in the zone of reduced efficiency according to Fig. 4. In such a situation, another type for capacitors or semiconductor switching elements should be chosen.

3 Experimental Results

To confirm the findings a series of experiments were carried out. The experimental equipment includes the specially made resonant circuit and WPT laboratory installation that are shown in Fig. 6. The voltage of WPT laboratory installation is rectangular pulses with adjustable duty cycle and adjustable pulse amplitude from 20 V to 540 V. Maximum permissible current of the installation is 60 A. The power capacity of the resonant circuit is 500 W and the input voltage is 24 V which corresponds to 1.15 Ω of the equivalent battery resistance. Resonant capacitors are realized as a set with a parallel-series connection consisting of 10 capacitors 75-715C50KTD17M5 with 1700 pF and 10 capacitors 75-715C50KTT56M5 with 560 pF.

The WPT laboratory installation is equipped with a wide range of measuring instruments, including a MY6243 digital LC-meter with an accuracy of ± 2%. When performing experiments, the inductances for each turn number obtained according to (9) and (10) were compared with the measured values. The discrepancy does not exceed 5% that is acceptable for further evaluation of the results and was caused by nonideality in the frame form and the winding pitch.

The turn number of the transmitting and receiving coils of the resonant circuit was chosen such that provide an extremum of wireless charger efficiency η. As seen from Fig. 4, the optimal inductance L is about 20 μH that corresponds to an intermediate turn number between two and three turns. It is most expedient to use three turns since in this case, the efficiency is close, but the current transmission ratio a_i is smaller which allows using transistors of a lower class in maximum current in the inverter, and also reducing the losses in the inverter and capacitors of the resonant circuit.

The conducted experiments included oscilloscopy of currents and voltages at the transmitting and receiving circuits. Fig. 7 shows oscilloscope patterns for the experimentally found resonant mode that point out to resonant frequency is 89.5 kHz.

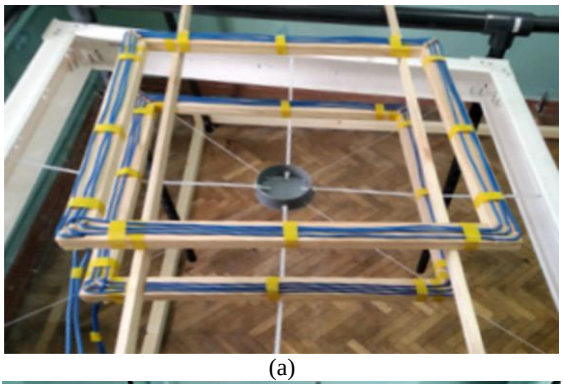

(a)

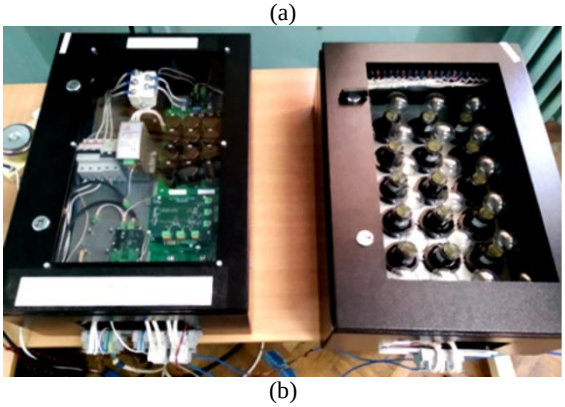

(b)

Fig. 6 The experimental equipment: a) resonant circuit and b) WPT laboratory installation.

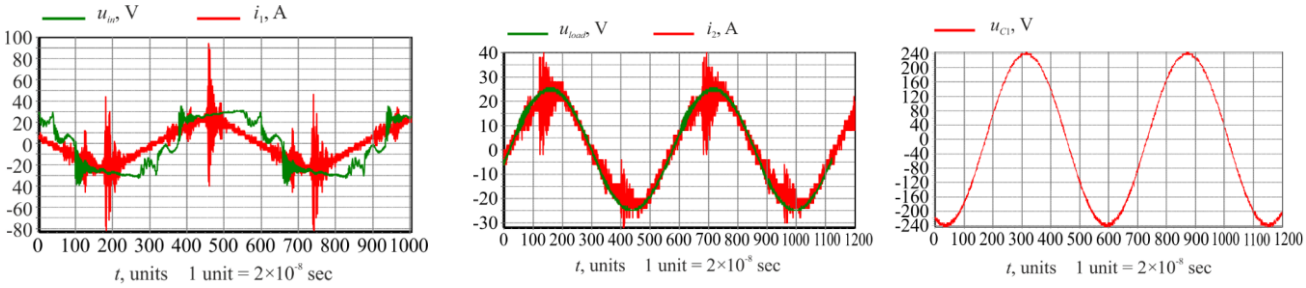

(a) (b) (c)

Fig. 7 Oscilloscope patterns of currents and voltages: a) on the inverter output; b) on R_{load}, and c) on the primary side capacitor.

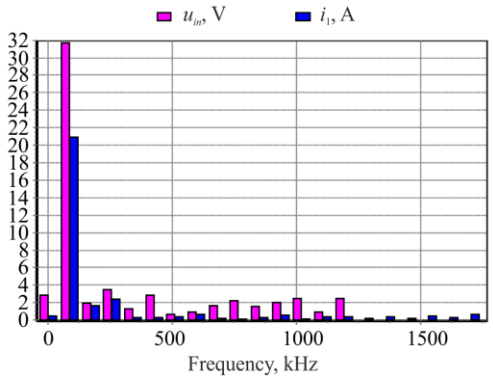

Fig. 8 Harmonic compositions of inverter output.

Table 3 Comparison of the criteria obtained in different ways.

The results obtained via	The criteria				
	η [%]	k_i [A/V]	k_{C1} [times]	k_{C2} [times]	a_i [times]
Parametric analysis	95.5	0.865	10.45	9.4	1.12
Experiment	87.6	0.82	7.51	5.35	1.13

The obtained resonant frequency indicates the 0.55% deviation from the designed value which confirms the correctness of the methods that were used to develop the coils. The currents and voltages have higher harmonics, which is due to the power transistors switching of the inverter in conjunction with parasitic inductances and capacities of the resonant circuit, that is especially expressed in the inverter output for which Fig. 8 shows the harmonic compositions. To gain an objective comparison of the experimental data with the results of parametric analysis, the criteria were determined via experiments in relation to the first harmonic.

Table 3 shows the criteria obtained experimentally for the first harmonic and calculated during parametric analysis. Comparison of these data certifies good convergence between the results obtained in different ways. The only parameters where deviation exceeded 5% are the efficiency and excess voltages on the resonant circuit capacitors over the input voltage. That may be caused by the losses in the capacitors and losses due to the current displacement effect that the mathematical model did not take into account, or by the possible asymmetry of the primary and secondary circuits due to the parameter imperfection of capacitors and coils. Nevertheless, the obtained discrepancies fall within the margin of error in engineering, therefore, the results of the parametric analysis could be reputed as experimentally confirmed.

4 Conclusions

The research results showed that the suggested set of criteria indicate the following:

1. When designing a wireless charger for unmanned electric vehicles with restrictions on the dimensions and the resonant frequency magnitude, the best energy efficiency can be achieved by selecting the optimal inductances and capacitances relation of the resonant circuit.
2. With the optimal parameters relation in terms of energy efficiency, there is a minimum overvoltage on the capacitors in the resonant circuits which allows using capacitors of the lower voltage class.
3. With an increase in the load at a given voltage, the energy efficiency of the resonant circuit appears at a lower inductance of the resonant circuit.

The described models, approaches, and parametric analysis underlie the flowchart based on these generalizations that can be used at the design stage to rational choosing of inductances and capacitances of the resonant circuit of the wireless charger.

Intellectual Property

The authors confirm that they have given due consideration to the protection of intellectual property associated with this work and that there are no impediments to publication, including the timing of publication, with respect to intellectual property.

Funding

This work was carried out as part of the scientific project “Development and research of the resonant DC/DC converter for unmanned technological electric vehicles” funded by a grant of Sevastopol State University.

CRediT Authorship Contribution Statement

V. Zavylov: Idea & Conceptualization, Methodology, Supervision. **I. Semykina:** Research & Investigation, Analysis, Revise & Editing. **S. Abeidulin:** Research & Investigation, Analysis, Verification. **E. Dubkov:** Research & Investigation, Software and Simulation, Data Curation. **A. H. Veliliaev:** Research & Investigation, Software and Simulation, Data Curation.

Declaration of Competing Interest

The authors hereby confirm that the submitted manuscript is an original work and has not been published so far, is not under consideration for publication by any other journal and will not be submitted to any other journal until the decision will be made by this journal. All authors have approved the manuscript and agree with its submission to "Iranian Journal of Electrical and Electronic Engineering".

References

[1] C. S. Wang, O. H. Stielau, and G. A. Covic, "Design considerations for a contactless electric vehicle battery charger," IEEE Transactions on Industrial Electronics, Vol. 52, No. 5, pp. 1308–1314, Oct. 2005.

[2] C. Qiu, K. T. Chau, C. Liu, and C. C. Chan, "Overview of wireless power transfer for electric vehicle charging," in *International Battery, Hybrid and Fuel Cell Electric Vehicle Symposium (EVS27)*, Barcelona, Spain, pp. 17–20, Nov. 2013.

[3] S. Obayashi, T. Shijo, M. Suzuki, W. H. Yang, Y. Kamiya, "85 kHz band 44 kW wireless rapid charging system for field test and public road operation of electric bus," *World Electric Vehicle Journal*, Vol. 10, No. 2, pp. 26, 2019.

[4] S. Li and C. C. Mi, "Wireless power transfer for electric vehicle applications," *IEEE Journal of Emerging and Selected Topics in Power Electronics*, Vol. 3, No. 1, pp. 4–17, Mar. 2015.

[5] Z. Jiali, Z. Bo, W. Xiao, D. Qiu, and Y. Chen, "Nonlinear parity-time-symmetric model for constant efficiency wireless power transfer: Application to a drone-in-flight wireless charging platform," *IEEE Transactions on Industrial Electronics*, Vol. 66, No. 5, pp. 4097–4107, May 2019.

[6] Z. Yan, Y. Zhang, T. Kan, F. Lu, K. Zhang, B. Song, and C. C. Mi, "Frequency optimization of a loosely coupled underwater wireless power transfer system considering eddy current loss," *IEEE Transactions on Industrial Electronics*, Vol. 66, No. 5, pp. 3468–3486, May 2019.

[7] C. Auvigne, P. Germano, Y. Civet, and Y. Perriard, "Design considerations for a contactless battery charger," in *16th European Conference on Power Electronics and Applications*, Lappeenranta, Finland, pp. 26, Aug. 2014.

[8] A. Khaligh and S. Dusmez, "Comprehensive topological analysis of conductive and inductive charging solutions for plug-in electric vehicles," *IEEE Transaction on Vehicular Technology*, Vol. 61, No. 8, pp. 3475–3489, Oct. 2012.

[9] S. Chatterjee, A. Iyer, C. Bharatiraja, I. Vaghasia, and V. Rajesh, "Design optimisation for an efficient wireless power transfer system for electric vehicles," in *1st International Conference on Power Engineering, Computing and Control*, VIT University, Chennai Campus, pp. 1015–1023, Mar. 2017.

[10] A. El-Shahat, E. Ayisire, Y. Wu, M. Rahman, and D. Nelms, "Electric vehicles wireless power transfer state-of-the-art," *Energy Procedia*, Vol. 162, pp. 24–37, Apr. 2019.

[11] A. Krainyukov, I. Lyaksa, and R. Saltanovs, "Research of the efficiency of the wireless power transfer with the employment of DD Inductance Coils," *Transport and Telecommunication*, Vol. 16, No. 4, pp. 341–352, 2015.

[12] M. Al-Saadi, A. Ibrahim, A. Al-Omari, A. Al-Gizi, and A. Craciunescu, "Analysis and comparison of resonance topologies in 6.6kw inductive wireless charging for electric vehicles batteries," in *12th International Conference Interdisciplinarity in Engineering*, No. 32, pp. 426–433, Oct. 2018.

[13] M. Simica, C. Bila, and V. Vojisavljevic, "Investigation in wireless power transmission for UAV charging," in *9th International Conference on Knowledge Based and Intelligent Information and Engineering Systems Procedia Computer Science*, No. 60, pp. 1846–1855, Sep. 2015.

[14] W. Huang and H. Ku, "Analysis and optimization of wireless power transfer efficiency considering the tilt angle of a coil," *Journal of Electromagnetic Engineering and Science*, Vol. 18, pp. 13–19, 2018.

[15] L. Tan, Z. Zhang, Z. Zhang, B. Deng, M. Zhang, J. Li, and X. Huang, "A segmented power-efficiency coordinated control strategy for bidirectional wireless power transmission systems with variable structural parameters," *IEEE Access*, Vol. 6, pp. 40289–40301, 2018.

[16] Y. Li, K. Song, Z. Li, J. Jiang, and Ch. Zhu, "Optimal efficiency tracking control scheme based on power stabilization for a wireless power transfer system with multiple receivers," *Energies*, Vol. 11, No. 5, pp. 1–18, 2018.

[17] L. Tan, M. Zhang, S. Wang, S. Pan, Z. Zhang, J. Li, and X. Huang, "The design and optimization of a wireless power transfer system allowing random access for multiple loads," *Energies*, Vol. 12, No. 6, pp. 1–19, 2019.

[18] "Wireless power transfer for light-duty plug-in/ Electric vehicles and alignment methodology," *SAE J2954*, SAE International: Warrendale, PA, USA, Apr. 2019.

[19] P. L. Kalantarov and L. A. Zeitlin, *Raschet induktivnostey: Spravochnaya kniga* [Calculation of inductance: A reference book]. Leningrad: Energoatomizdat, 1986.

[20] M. F. Iskander, *Electromagnetic fields and waves*. Englewood Cliffs: Prentice-Hall, 1992.

[21] I. Semykina, V. Zavyalov, and V. Krylov, "Research of the laboratory prototype for the battery charging system based on wireless power transfer," in *21st International Conference of Young Specialists on Micro/Nanotechnologies and Electron Devices*, Novosibirsk State Technical University, Russia, pp. 324–330, 2020.

[22] D. M. Vilathgamuwa, and J. P. K. Sampath, "Wireless power transfer (WPT) for electric vehicles (EVs) – Present and future trends," in *Plug in Electric Vehicles in Smart Grids: Integration Techniques*, A. Ghosh, F. Shahnia, and S. Rajakaruna, Eds. Singapore: Springer, pp. 33-60, 2015.

V. M. Zavyalov was born in 1974. He received the Ph.D. in 2003 and D.Sc. 2009 degrees in Electrotechnical Complexes and Systems from Kuzbass State Technical University (KuzSTU). From 1998 to 2014, he worked at KuzSTU, then from 2014 to 2018, he was the director of the Institute of Power Engineering at Tomsk Polytechnic University. Nowadays he has been working as the head of the Department "Power Systems of Nuclear Stations" at Sevastopol State University. He is the author of the book, more than 100 articles, and 3 inventions. His area of scientific interests includes control of electromechanical transformation of energy, identification of parameters and condition of electric drives, dynamic loadings decrease in mechanical transfers by means of the adjustable electric drive; spatial electric drives in robotics and electric vehicles. Dr. Zavyalov was the operations director of several research and development projects. He is a member of the dissertation council D 121.102.01 at T.F. Gorbachev Kuzbass State Technical University and an accredited expert of the Russian Federal Roster of Scientific and Technical Experts.

I. Y. Semykina was born in 1984. She graduated from Kuzbass State Technical University in 2005 and received D.Sc. in Electrotechnical Complexes and Systems from Tomsk Polytechnic University in 2014. Dr. Semykina works as the director of the Educational and Scientific Center of Information Technologies for Education at Sevastopol State University. Her scientific interests include energy saving, electrical equipment, automation, control of complex dynamic systems, and electrical engineering. She is the author of 125 publications including 4 inventions, 1 utility model patent, and 3 computer programs. Dr. Semykina is a member of the dissertation council D 121.102.01 at T.F. Gorbachev Kuzbass State Technical University. She is the area editor of the scientific journal "Energy Web and Information Technologies".

S. A. Abeidulin was born in 1971. He received his Dipl.-Ing. in Electrical Engineering from the Sevastopol National University of Nuclear Energy and Industry in 1998 and worked here till 2014. In 2011 he received his master's degree. From 2014 he has been working as a senior lecturer at the department "Power Systems of Nuclear Stations" of Sevastopol State University. Mr. Abeidulin is the author of 10 teaching aids and 5 articles. His research interests are electrical engineering and power engineering, electric drive and its control, electric power converters, wireless power transfer.

E. A. Dubkov was born in 1984. He gets Dipl.-Ing. in Electrical Engineering in 2006 and master's degree in 2008. From 2007 to nowadays he has been working at the Sevastopol State University in the Institute of Nuclear Energy and Industry at the department "Power Systems of Nuclear Stations" as a senior lecturer. He is the author of more than 10 articles. The research interests are the control systems of electromechanical energy conversion, the electrical part of thermal and nuclear power plants.

A. S. Veliliaev was born in 1999. Received his bachelor's degree in Electricity and Electrical Engineering in 2020 at the Sevastopol State University. From 2020 he has been working as an engineer at the department "Power Systems of Nuclear Stations" of the same university. He also participates in the grant project "Development of competitive technologies for the creation of components for a mobile photovoltaic installation of high efficiency".